

## OPEN ACCESS

## EDITED BY

Trude Helen Flo,  
Norwegian University of Science and  
Technology, Norway

## REVIEWED BY

Ranjeet Kumar,  
The State University of New Jersey,  
United States  
Roberto Zenteno-Cuevas,  
Universidad Veracruzana, Mexico  
Norbert Reiling,  
Research Center Borstel (LG), Germany

## \*CORRESPONDENCE

Anna Allué-Guardia  
✉ aallueguardia@txbiomed.org  
Jordi B. Torrelles  
✉ jtorrelles@txbiomed.org

RECEIVED 08 December 2023

ACCEPTED 13 February 2024

PUBLISHED 04 March 2024

## CITATION

Allué-Guardia A, Garcia-Vilanova A,  
Schami AM, Olmo-Fontáñez AM, Hicks A,  
Peters J, Maselli DJ, Wewers MD, Wang Y and  
Torrelles JB (2024) Exposure of  
*Mycobacterium tuberculosis* to human  
alveolar lining fluid shows temporal and  
strain-specific adaptation to the lung  
environment. *Front. Tuberc.* 2:1352806.  
doi: 10.3389/ftubr.2024.1352806

## COPYRIGHT

© 2024 Allué-Guardia, Garcia-Vilanova,  
Schami, Olmo-Fontáñez, Hicks, Peters,  
Maselli, Wewers, Wang and Torrelles. This is an  
open-access article distributed under the  
terms of the [Creative Commons Attribution  
License \(CC BY\)](https://creativecommons.org/licenses/by/4.0/). The use, distribution or  
reproduction in other forums is permitted,  
provided the original author(s) and the  
copyright owner(s) are credited and that the  
original publication in this journal is cited, in  
accordance with accepted academic practice.  
No use, distribution or reproduction is  
permitted which does not comply with these  
terms.

# Exposure of *Mycobacterium tuberculosis* to human alveolar lining fluid shows temporal and strain-specific adaptation to the lung environment

Anna Allué-Guardia<sup>1\*</sup>, Andreu Garcia-Vilanova<sup>1</sup>,  
Alyssa M. Schami<sup>1,2</sup>, Angélica M. Olmo-Fontáñez<sup>1,2</sup>,  
Amberlee Hicks<sup>1</sup>, Jay Peters<sup>3</sup>, Diego J. Maselli<sup>3</sup>,  
Mark D. Wewers<sup>4</sup>, Yufeng Wang<sup>5</sup> and Jordi B. Torrelles<sup>1,6\*</sup>

<sup>1</sup>Population Health Program, Tuberculosis Group, Texas Biomedical Research Institute, San Antonio, TX, United States, <sup>2</sup>Integrated Biomedical Sciences Program, University of Texas Health Science Center at San Antonio, San Antonio, TX, United States, <sup>3</sup>Division of Pulmonary and Critical Care Medicine, School of Medicine, UT Health San Antonio, San Antonio, TX, United States, <sup>4</sup>Department of Internal Medicine, Pulmonary, Critical Care and Sleep Medicine Division, College of Medicine, The Ohio State University, Columbus, OH, United States, <sup>5</sup>Department of Molecular Microbiology and Immunology, South Texas Center for Emerging Infectious Diseases, University of Texas at San Antonio, San Antonio, TX, United States, <sup>6</sup>International Center for the Advancement of Research and Education (I-CARE), Texas Biomedical Research Institute, San Antonio, TX, United States

Upon infection, *Mycobacterium tuberculosis* (*M.tb*) reaches the alveolar space and comes in close contact with the lung mucosa or human alveolar lining fluid (ALF) for an uncertain period of time prior to its encounter with alveolar cells. We showed that homeostatic ALF hydrolytic enzymes modify the *M.tb* cell envelope, driving *M.tb*-host cell interactions. Still, the contribution of ALF during *M.tb* infection is poorly understood. Here, we exposed 4 *M.tb* strains with different levels of virulence, transmissibility, and drug resistance (DR) to physiological concentrations of human ALF for 15-min and 12-h, and performed RNA sequencing. Gene expression analysis showed a temporal and strain-specific adaptation to human ALF. Differential expression (DE) of ALF-exposed vs. unexposed *M.tb* revealed a total of 397 DE genes associated with lipid metabolism, cell envelope and processes, intermediary metabolism and respiration, and regulatory proteins, among others. Most DE genes were detected at 12-h post-ALF exposure, with DR-*M.tb* strain W-7642 having the highest number of DE genes. Interestingly, genes from the KstR2 regulon, which controls the degradation of cholesterol C and D rings, were significantly upregulated in all strains post-ALF exposure. These results indicate that *M.tb*-ALF contact drives initial bacterial metabolic and physiologic changes, which may have implications in the early events of *M.tb* infection.

## KEYWORDS

*Mycobacterium tuberculosis*, alveolar lining fluid, lung mucosa, transcriptomics, cell envelope

## Introduction

Airborne pathogen *Mycobacterium tuberculosis* (*M.tb*) is the causative agent of tuberculosis (TB), one of the top leading causes of death worldwide due to a single infectious agent, with 11 million cases and ~1.6 million attributed deaths in 2021 and many underreported diagnoses due to the coronavirus disease 2019 (COVID-19) pandemic disruptions in global healthcare (1). Indeed, a 20% raise in the number of TB deaths is predicted over the next 5 years, resulting in a setback of at least 5 to 8 years in End-TB Strategy (2, 3). Further, relocation of resources and access limitations to healthcare during the COVID-19 pandemic predict an increase in the number of drug-resistant (DR) TB cases worldwide (4).

During the process of natural infection, *M.tb* is initially deposited in the lung alveolar space where it first encounters the lung mucosa, composed of a surfactant lipid layer and an aqueous hypophase (called alveolar lining fluid or ALF). *M.tb* is thought to be in close contact with ALF for an undefined period (from min to h) before encountering host alveolar resident cells and after its escape from dying cells during the initial phases of infection, where it can interact with ALF innate soluble components (5). Specifically, homeostatic hydrolytic activities (hydrolases) present in human ALF, whose main function is ALF degradation and recycling, alter the *M.tb* cell envelope upon ALF-*M.tb* exposure in as little as 15 min (6). These ALF-induced cell envelope alterations in *M.tb* are shown to influence subsequent interactions with immune host cells *in vitro* and *in vivo*, ultimately determining the infection outcome (6–12). Indeed, exposure to ALF resulted in decreased association and intracellular growth of *M.tb* in human macrophages, as well as increased *M.tb* intracellular killing in neutrophils while limiting tissue damage, overall leading to a better control of the infection by professional phagocytes (6, 8). In addition to ALF hydrolases, levels and functionality of other ALF soluble components are significantly altered in some human populations such as the elderly, resulting in accelerated *M.tb* growth *in vitro* (human macrophages and alveolar epithelial cells) and exacerbated infection *in vivo* in young mice when *M.tb* is exposed to elderly ALF (10, 12, 13). Thus, the host ALF status and functionality might play an important role in shaping the *M.tb* cell envelope during the initial stages of the infection (10, 13). However, the overall impact of the ALF on the adaptation of *M.tb* to the alveolar space prior to being recognized by host cells and subsequent infection is still largely unknown.

Biochemical studies have also determined that the *M.tb* cell envelope composition is quite diverse between phylogenetic lineages and/or geographical regions, and even among strains with different drug resistance patterns (14–17), which can lead to different interactions with host immune cells (18). Still, it is uncertain if different *M.tb* strains/lineages exposed to human ALF will have distinct metabolic responses prior to encountering host cells.

In this study, we aimed to determine the overall and strain-specific effects of human ALF exposure on different *M.tb* genomic backgrounds driving *M.tb*-host interactions (6–12). For this, we selected four well-characterized *M.tb* strains, two from lineage 4 ( $H_{37}R_v$  and CDC1551, European, American, and African) and two from lineage 2 (HN878 and W-7642, Beijing/East-Asian). Besides

their lineage, *M.tb* strains were also selected based on their levels of transmissibility, virulence, and drug resistance.  $H_{37}R_v$  is a common reference laboratory strain derived from a patient with chronic pulmonary TB at the beginning of the 20th century and selected for its virulence in animal models (19). CDC1551 is a clinical strain isolated from a TB outbreak in the mid-90s in a small rural area close to the Kentucky-Tennessee border. This strain is considered of low virulence but highly transmissible in humans (20). Though highly immunogenic at early stages of infection, CDC1551 is efficiently controlled in the lungs of infected animals (21). Strain HN878 was isolated during a TB outbreak in Houston, Texas, during the late 90s (22). Its hypervirulent phenotype is attributed to the presence of cell envelope phenolic glycolipids (PGLs) and triglycerides, and is associated with a rapid bacterial growth and reduced survival due to decreased TH1 host protective immunity driving cavitary disease (23). Finally, W-7642 was isolated in the early 90s after a series of outbreaks in New York City caused by the spread of a multidrug resistant (MDR)-*M.tb* Beijing clone. This strain is also considered highly virulent, since it caused increased mortality rates when compared to other clinical isolates (24).

Thus, in order to define the metabolic adaptations of these four *M.tb* strains to the human ALF environment, we performed RNA sequencing after their exposure to human ALF, and determined shared and strain-specific differentially expressed genes between strains when compared to unexposed bacteria (Supplementary Figure S1). Our results indicate that time-dependent exposure of *M.tb* to ALF drives global metabolic and physiologic changes in *M.tb* with potential implications in bacterial recognition by host cells and the establishment and outcome of the infection.

## Materials and methods

### Human subjects and ethics statement

Blood and bronchoalveolar lavage fluid (BALF) was collected from healthy adult volunteers, in strict accordance with the US Code of Federal Regulations and approved Local Regulations (The Ohio State University Human Subjects IRB numbers 2008H0135 & 2008H0119 and Texas Biomedical Research Institute/UT-Health San Antonio Human Subjects IRB numbers HSC20170667H & HSC20170315H), and Good Clinical Practice as approved by the National Institutes of Health (NIAID/DMID branch), with written informed consent from all human subjects. Healthy adult volunteers (18–45 years old) were TST- or IGRA-negative and were recruited from both sexes (50:50 male:female ratio) with no discrimination based on race or ethnicity. The following comorbidities were excluded: drug and alcohol users, smokers, asthma, acute pneumonia, upper/lower respiratory tract infections, acute illness/chronic condition, heart disease, diabetes, obesity, obstructive pulmonary disease (COPD), renal failure, liver failure, hepatitis, thyroid disease, rheumatoid arthritis, immunosuppression or taking nonsteroidal anti-inflammatory agents, human immunodeficiency virus (HIV)/AIDS, cancer requiring chemotherapy, leukemia/lymphoma, seizure history, blood disorders, depression, lidocaine allergies (used during

the BAL procedure), pregnancy, nontuberculous mycobacterial infection, and TB.

## Collection of BALF and ALF isolation

BALF was collected from healthy adult donors in 80 mL of sterile endotoxin-free human isotonic saline (0.9% NaCl), filtered through 0.2  $\mu$ m filters, and concentrated 20-fold using Amicon Ultra Centrifugal Filter Units with a 10-kDa molecular mass cutoff membrane (Millipore Sigma, Burlington, MA, USA) to obtain the ALF physiological concentration within the lung (1 mg/mL of phospholipid), as we described (6–13, 25). We use the *in vivo* relevant levels of 0.5 to 1.5 mg/ml of surfactant phospholipids in the lung mucosa (26), measured by phospholipid assay (27). The 20-fold concentration process removes free surfactant lipids and free fatty acids of <10-kDa, leaving functional hydrolases and other proteins such as surfactant proteins A and D (SP-A/SP-D), complement, and antimicrobial peptides in the ALF fraction, as well as other molecules of >10-kDa such as cholesterol. Effective lipid removal (<10-kDa) from ALF was confirmed in previous studies by mass spectrometry (MS) of fatty acid methyl ester (FAMES) derivatives (6). ALF was then aliquoted and stored at  $-80^{\circ}\text{C}$  until further use. Samples were maintained at  $4^{\circ}\text{C}$  on ice and in endotoxin-free sterile conditions during the whole procedure.

## Bacterial cultures and ALF exposure

*M.tb* strains CDC1551, H<sub>37</sub>R<sub>v</sub> (ATCC# 25618), HN878 (BEI Resources, NR-13647), and W-7642 were cultured from frozen stocks in 7H11 agar plates (BD BBL), supplemented with oleic acid, albumin, dextrose and catalase (OADC) for 14 days at  $37^{\circ}\text{C}$ . Single bacterial suspensions in 0.9% NaCl were obtained as described (6–12, 25), and bacterial pellets ( $\sim 1 \times 10^9$  bacteria/ml) obtained after centrifugation (13,000  $\times g$ , 10 min) were further incubated in a 50  $\mu$ l pool of ALFs (mixture of ALFs from  $n = 17$  different donors in equal proportions), 50:50 male:female ratio, no discrimination in ethnicity and race) for 15 min or  $\sim 12$  h at  $37^{\circ}\text{C}$  (no agitation). After exposure, ALF was removed and bacterial pellets washed with 0.9% NaCl. Pellets were further incubated in RNAProtect (Qiagen, Hilden, Germany) for 10 min at room temperature (RT), centrifuged at 13,000  $\times g$  and stored at  $-80^{\circ}\text{C}$  until further use. For each of the strains, unexposed bacteria were processed in parallel and used as controls (bacterial pellets incubated for 15 min or  $\sim 12$  h at  $37^{\circ}\text{C}$  without ALF). Two independent experiments were performed: two different exposures to the same pool of ALFs on different days, using single bacterial suspensions of newly fresh harvested bacteria grown in 7H11 agar for each strain studied.

## RNA extraction, library prep and RNA sequencing

Stored bacterial pellets were used for RNA extraction using the Quick-RNA Fungal/Bacterial Miniprep kit (Zymo Research,

Irvine, CA, USA), following the manufacturer's protocol. Briefly, bacterial pellet was resuspended in lysis buffer and transferred to a ZR BashingBead Lysis tube containing 0.1 mm and 0.5 mm ceramic beads. A bead beating procedure to break the mycobacterial cell envelope was performed in a BioSpec Mini-Beadbeater-24 (six cycles of 45 s at 3,800 rpm, with 3 min intervals on a cooler rack). RNA in the supernatant was isolated using Zymo-spin columns, with an in-column DNase I treatment, and eluted in nuclease-free water. A second DNase treatment was performed on the isolated RNA using the TURBO DNase reagent (Thermo Fisher Scientific, Waltham, MA, USA), and RNA was further purified using the RNA Clean & Concentrator kit (Zymo Research, Irvine, CA, USA). RNA final concentration was measured with a Qubit 4 Fluorometer using the HS RNA kit (Thermo Fisher Scientific, Waltham, MA, USA), and RIN numbers were obtained using the 4200 TapeStation System (Agilent, Santa Clara, CA, USA) to determine RNA quality before sequencing. A stranded whole transcriptome RNA library was constructed using the Zymo-Seq RiboFree Total RNA kit (Zymo Research) following the manufacturer's guidelines. RNA (500 ng) was used as input to construct the library, which included a rRNA depletion step of 30 min followed by 14 cycles of PCR. A 75-bp paired-end (PE) sequencing was conducted using a NextSeq 500 Mid Output Illumina platform, obtaining 5–8 million PE reads per sample. All samples (from  $n = 2$  independent experiments) were sequenced in the same flow cell to avoid sequencing batch effects.

## Data analysis

Raw reads were trimmed (phred score of 30) and aligned to the reference genome H<sub>37</sub>R<sub>v</sub> (Genbank NC\_000962.3) (28) using STAR v2.5.3a with default values in the Partek Flow Genomic Analysis software (v9.0.20.0202, Partek Inc., Chesterfield, MO, USA). Further analyses were performed in the iDEP.94 software (<http://bioinformatics.sdstate.edu/idep94/>) (29): first, uploaded read count raw data were filtered (0.5 CPM,  $n = 1$  library) to remove lowly expressed genes and transformed with edgeR as  $\log_2$  (CPM + c) using default settings (30), and used for clustering and principal component Analysis (PCA). Hierarchical clustering of normalized gene expression levels was calculated using default values (correlation distance, average linkage, cutoff Z score of 4), and shown as a heatmap. Then, significant differentially expressed genes (DEGs) between ALF-exposed *M.tb* and unexposed *M.tb* (control) for each of the strains and time points were identified using the DESeq2 method (31) in iDEP.94, with an FDR cutoff of 0.1 and a minimum fold change (FC) of 2 (corresponding to a  $\log_2$  FC equal or greater than an absolute value of 1). The Benjamini-Hochberg procedure was used to adjust the false discovery rate (FDR), and fold changes were calculated using an Empirical Bayes shrinkage approach (31) and the Wald test implemented in DESeq2. Functional categories for DEGs were extracted from Mycobrowser (32). Gene enrichment analysis was performed in ShinyGO 0.77 using default settings (FDR cutoff of 0.05 and minimum pathway size of 2, Pathway database: all available gene sets) (33). A summary of the experimental conditions and workflow used for RNA sequencing and data analysis is shown in [Supplementary Figure S1](#).

## Validation of gene expression by RT-qPCR

Some of the genes that were differentially expressed were selected for validation using RT-qPCR (Supplementary Table S1). Selection criteria was based on genes discussed more in detail in the manuscript, belonging to different pathways and/or categories, and that showed significant differences between strains and/or time points (*echA20*, *KstR2*, *mymA*, *papA1*, *papA3*, *mmpL10*, *mmpL8*, *mprA*, *sigF*, *espC* and *esxH*). Strains selected for RT-qPCR were the ones that showed the most differential expression for each of the genes. Briefly, 500 ng of RNA (same RNA that was used for RNA-seq) were used for the synthesis of cDNA using the RevertAid H Minus First Strand cDNA Synthesis kit (Thermo Fisher Scientific, Waltham, MA, USA) with random hexamer primers, following the manufacturer's instructions. Then, cDNA and specific primers were used in a 20  $\mu$ l qPCR reaction with PowerUp SYBR Green Master Mix (Applied Biosystems, Waltham, MA, USA) run in an Applied Biosystems 7500 Real-Time PCR instrument with the following settings: reporter SYBR Green, no quencher, passive reference dye ROX, standard ramp speed, and continuous melt curve ramp increment, as described (25). Relative expression was calculated using the  $2^{-\Delta\Delta CT}$  method (34) with *sigA* as the housekeeping gene.

## Statistical analyses

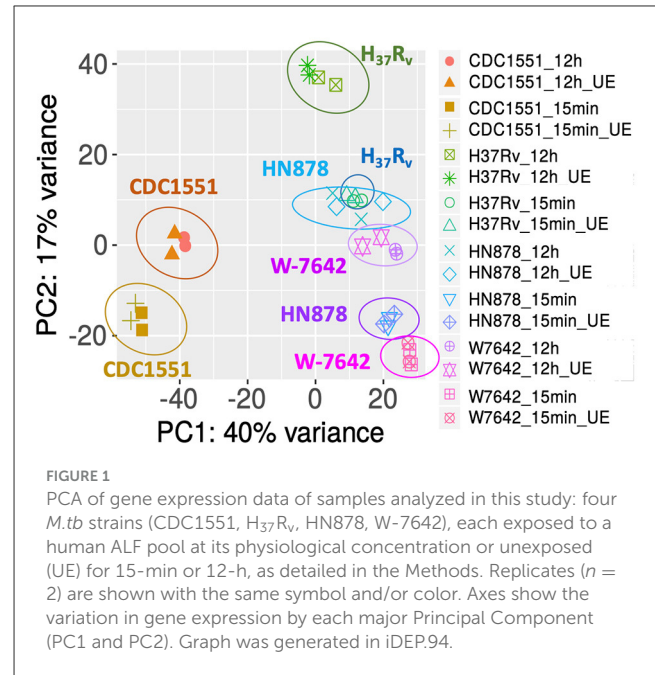
Statistical significance for bacterial uptake and intracellular growth rate was determined by multiple paired Student's *t* tests (ALF-exposed vs. unexposed *M.tb*). A 2-way ANOVA for multiple comparisons with an uncorrected Fisher's LSD test and main effects model was used for qPCR data ( $\Delta$ Ct ALF-exposed vs.  $\Delta$ Ct unexposed *M.tb* for each of the strains and time points).

## Results

### Alignment statistics, PCA, and clustering of samples

RNA from four *M.tb* strains (*H37Rv*, CDC1551, HN878, and W-7642) exposed to human ALF for 15-min and 12-h was extracted and sequenced. The total average number of reads/sample after removing low quality reads during the initial quality control (QC) was 6.15 million, ranging from  $\sim$  4.1 to 11.3 million. The number of aligned reads to the *M.tb* reference genome was  $\sim$  90% on average. Samples with  $<$ 70% of aligned reads were analyzed using Kraken (35) to discard potential sample contamination (data not shown). All samples had a coverage of more than 97% of their genome after alignment, with GC content of 62%. A Pearson correlation matrix was computed, showing a correlation of more than  $r = 0.97$  between sample replicates (Supplementary Figure S2A). Our quality post-alignment statistics and quality control metrics are found in Supplementary Table S2.

Raw aligned data was then transformed and used for sample clustering and Principal Component Analysis (PCA). PCA grouped the samples based on *M.tb* strain (CDC1551, *H37Rv*, HN878, W-7642) and incubation time (15-min and 12-h), the main sources of variance in this dataset, indicating temporal and strain-specific



changes in transcriptional profiles of *M.tb* both before and after ALF exposure (Figure 1). Strain CDC1551 was furthest from the others at both time points tested, suggesting a more distinct transcriptional profile regardless of ALF exposure. We note here that the exposure time (15-min vs. 12-h) seems to have a bigger effect on the strains' transcriptome than the ALF exposure itself, since ALF-exposed and unexposed conditions are closely grouped in all the strains and time points. This indicates that the act of going from agar plates to being in suspension is causing a great number of transcriptional changes in *M.tb*, as one would expect. For this reason, unexposed bacteria was processed in parallel for each of the time points and used as control/baseline, and differential expression analyses were focused on the effects of ALF exposure (ALF-exposed vs. unexposed *M.tb*) at each time point rather than comparing exposure times.

Hierarchical clustering of normalized gene expression classified the samples in four main clusters (Supplementary Figure S2B). Cluster 1 (HN878 and W-7642 at 15-min) was closest to cluster 2 (HN878 and W-7642 at 12-h), indicating that those two strains presented the most similar transcriptional profile at each of the time points tested. They were followed by *H37Rv* at both time points (cluster 3) and CDC1551 (cluster 4), furthest from the others.

### Functional categories and enrichment of differentially expressed genes (DEGs)

We performed DE analysis of ALF-exposed vs. unexposed *M.tb* for each of the strains at both time points. A total of 397 DEGs were identified, with DR-*M.tb* strain W-7642 being the one with the most transcriptional changes after exposure to ALF for 12-h (152 downregulated and 87 upregulated genes) compared to unexposed bacteria (Figure 2A). Exposure for 15-min to ALF resulted only in a few DEGs: 32 in CDC1551, 12 in *H37Rv*, 9 in HN878, and

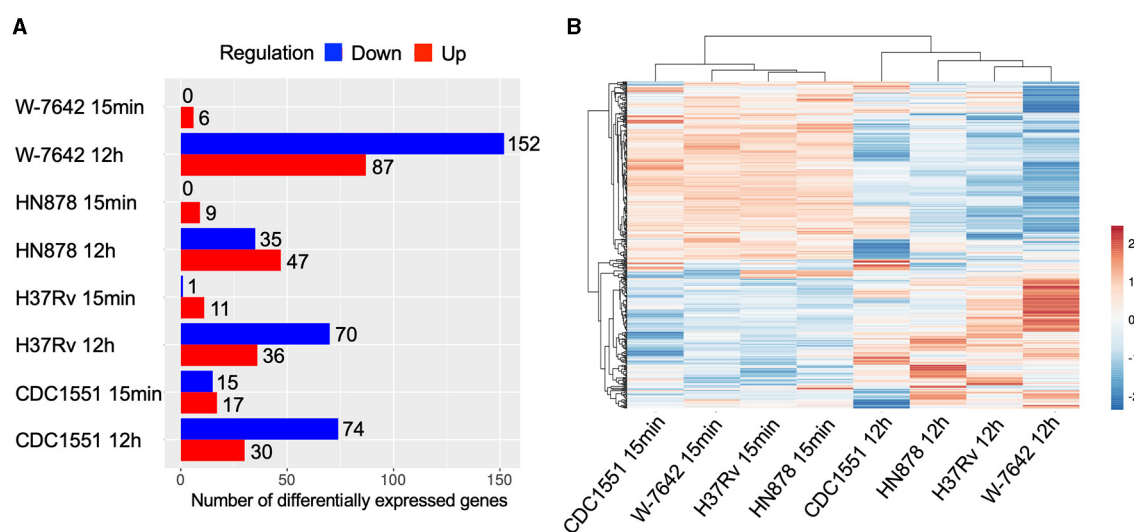


FIGURE 2

Differential expression analysis (ALF-exposed *M.tb* vs. unexposed *M.tb*) was performed for each of the strains (CDC1551, H<sub>37</sub>R<sub>v</sub>, HN878, W-7642) and time points (15-min and 12-h) using the DeSeq2 method in the iDEP.94 software, with the following settings: log<sub>2</sub>FC greater than an absolute value of 1, FDR < 0.1. (A) Number of differentially expressed genes (upregulated in red, downregulated in blue) for each of the strains and time points. Graph was generated in iDEP.94. (B) A heatmap of DEGs was constructed using the log<sub>2</sub>FC values in ClustVis (<https://bit.cs.ut.ee/clustvis/>) (36) with default settings (average correlation clustering), showing separation of strains in two major clusters based on ALF exposure time. Upregulated genes: orange; downregulated genes: blue.

6 in W-7642. Hierarchical clustering using DEGs clearly classified our samples in two main clusters based on the ALF exposure time (15-min vs. 12-h) (Figure 2B), indicating a temporal adaptation to the lung mucosa, with a much greater number of DEGs at 12-h compared to 15-min.

Identified DEGs belonged to different functional categories, including but not restricted to: conserved hypotheticals, intermediary metabolism and respiration, cell wall and cell processes, virulence, detoxification and adaptation, lipid metabolism, PE/PPE, information pathways, and regulatory proteins (Figure 3, Supplementary Table S3). At 15-min post-ALF exposure, the few DEGs found were associated to either lipid or intermediate metabolism, respiration, regulatory proteins or cell wall processes, except for strain CDC1551 which had more DEGs compared to the other strains and included other categories such as information pathways and PE/PPE (Supplementary Figure S3). At 12-h after ALF exposure, DEGs belonged to additional categories like virulence, detoxification and host adaptation, as well as insertion sequences and mobile genetic elements (MGEs) (Supplementary Figure S3).

We next performed gene enrichment analysis for the 397 total identified DEGs, and found 17 significantly enriched GO terms, including response to environmental pH, fatty acid biosynthetic process and lipid transport and associated beta-ketoacyl synthase activity, acyl transferase activity, cholesterol metabolic process, and mycofactocin and heme activity (Figure 4). Other enriched GO terms that did not pass the FDR cutoff of 0.05 were sulfolipid metabolic process, protein secretion by type VII secretion system, PPE superfamily, lipid biosynthesis, response to temperature and hypoxia, sigma factor activity, and phenolic phthiocerol biosynthetic process, among others (Supplementary Table S4).

## Exposure to ALF activates the KstR2 regulon associated with cholesterol utilization in *M.tb*

The cholesterol catabolic pathway is highly conserved in mycolic acid-containing actinomycetes, and is encoded by more than 100 genes in *M.tb* (37). There are three distinct sub-pathways or processes during cholesterol catabolism, according to the three parts of the molecule: side chain degradation, A & B ring degradation, and C & D ring degradation (38). Two major regulons, controlled by two TetR-type transcriptional regulators, have been associated with these processes: KstR1 regulates the transcription of side chain and A & B ring degradation genes, while KstR2 controls the transcription of C & D ring degradation genes (39). Other genes though to be regulated by cholesterol belong to the mammalian cell-entry Mce3R regulon, implicated in stress resistance (40), and the SigE regulon, essential for virulence (41).

Our results indicate that most KstR2 genes (12/15) were significantly upregulated (Log<sub>2</sub>FC > 1 and FDR < 0.1) either at 15-min or 12-h post-ALF exposure or both time points in one or more of the *M.tb* strains tested, with the exception of strain W-7642, where none of the KstR2 genes reached significant upregulation at 15-min (Figure 5, Supplementary Table S3). This included the genes for C & D ring degradation (3 out of 5 genes were significantly upregulated in at least one of the strains/conditions tested). In contrast, genes associated with the KstR1 regulon, including ATP-dependent cholesterol import genes encoded by the Mce4 transport system (42) and side chain and A&B ring degradation genes, were not differentially expressed when compared to unexposed *M.tb* at any of the ALF exposure periods of time tested (Supplementary Table S3).

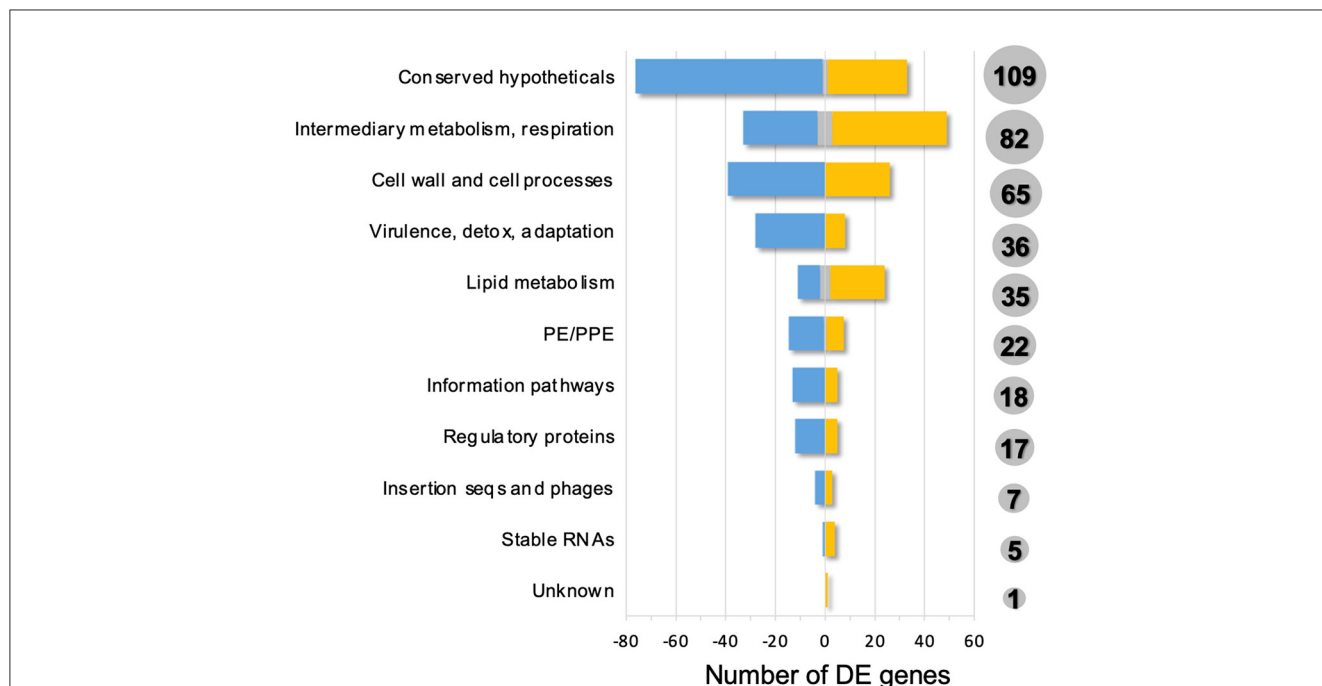


**FIGURE 3** Functional categories of differentially expressed genes (ALF-exposed *M.tb* vs. unexposed *M.tb*) found in this study. A total of 397 DEGs were classified into 11 functional categories, as defined in Mycobrowser. Total number of DEGs are shown in gray circles for each functional category. Upregulated DEGs in one or more strains: yellow; downregulated DEGs in one or more strains: blue; up or downregulated DEGs depending on the strain: gray.

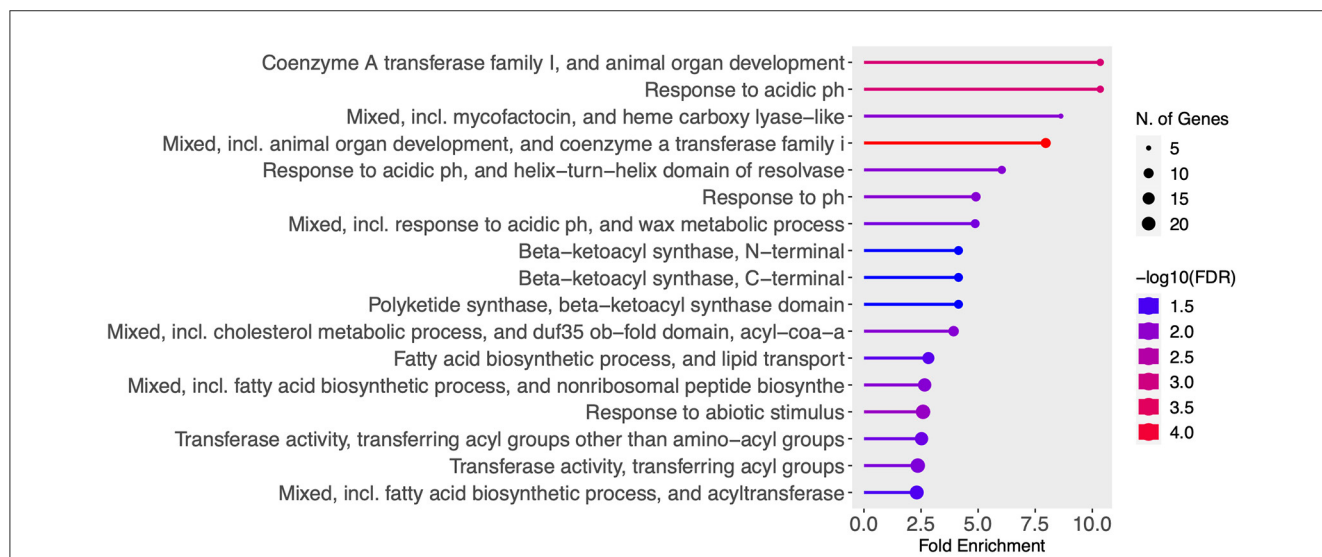
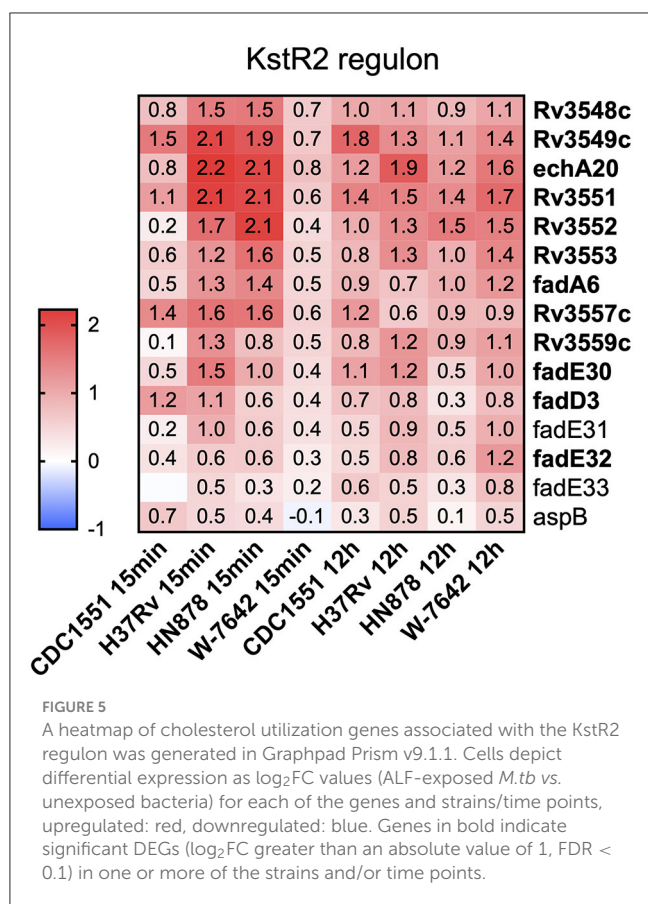


**FIGURE 4** Gene enrichment analysis of all 397 identified DEGs was performed in ShinyGO 0.77 using default settings: FDR cutoff of 0.05, minimum pathway size of 2, Pathway database—all available gene sets. Significant enriched GO terms (FDR <0.05) were sorted by fold enrichment and are shown. Graph color depicts significance [-log10 (FDR)] and the number of DEGs belonging to each enriched pathway is shown in proportional circles.

Only *ltp3* from the KstR1 regulon, encoding a keto acyl-CoA thiolase involved in the cholesterol side chain degradation (43), was significantly downregulated in strain CDC1551 at 12-h post-ALF exposure. Other significant DEGs associated with cholesterol side chain degradation were *fadE30*, *fadE32*, *echA20*, and *fadA6* (all upregulated and controlled by KstR2), and *fadB2* (downregulated in all four strains after 12-h of ALF exposure)

(Supplementary Table S3). In addition, of the 23 genes associated with the Mce3R regulon, only two were significantly differentially expressed: *yrbE3B*, encoding a hypothetical membrane protein with phospholipid transport activity, was upregulated in strain HN878 at 12 h post-exposure, while *mce3F* was downregulated in H<sub>37</sub>R<sub>v</sub> and W-7642 at that same time point (Supplementary Table S3). None of the cholesterol-associated *sigE* regulon genes were



differentially expressed in our dataset under the experimental conditions tested.

## Exposure to ALF shows a temporal adaptation of *M.tb* to the lung mucosa

In addition to the cholesterol utilization pathways, most *M.tb* strains showed upregulation of genes required for maintaining an appropriate mycolic acid layer composition and permeability of the *M.tb* cell envelope at 15 min post-ALF exposure, achieving statistical significance in strains CDC1551 and W-7642 (Figure 6, Supplementary Table S3). This included shared genes *Rv3083* (*mymA*), *Rv3084* (*lipR*), and *Rv3085* (*sadH*), as well as *Rv3086* (*adhD*), *Rv3087*, and *Rv3088* (*tgs4*), only significant in W-7642. In contrast, these genes were downregulated after 12 h of ALF exposure (Figure 7A). All these genes belong to the *mymA* operon, associated with maintaining the *M.tb* cell envelope under harsh conditions (44, 45).

At 12-h post-ALF exposure, we found several up and downregulated genes shared among two or more of the *M.tb* strains evaluated. Interestingly, both hypervirulent HN878 and drug resistant W-7642 showed significant upregulation of diacyltrehalose (DAT), penta-acyltrehalose (PAT) and sulfolipid-1 (SL-1) biosynthesis and transport genes *pks4*, *papA3*, *mmpL10*, *papA1*, and *mmpL8* (Figure 7B). These glycolipids are major *M.tb* cell envelope components (46), and some of them are significantly

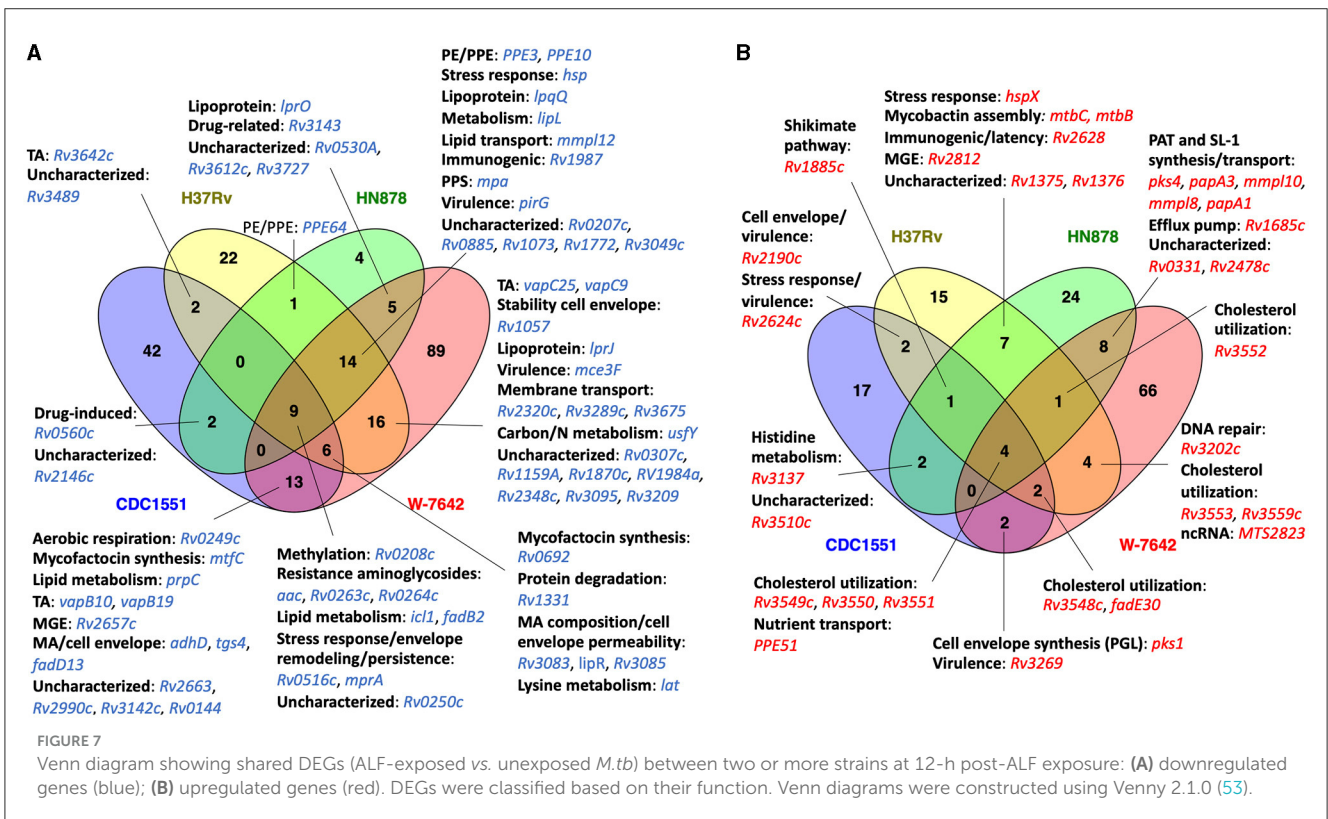
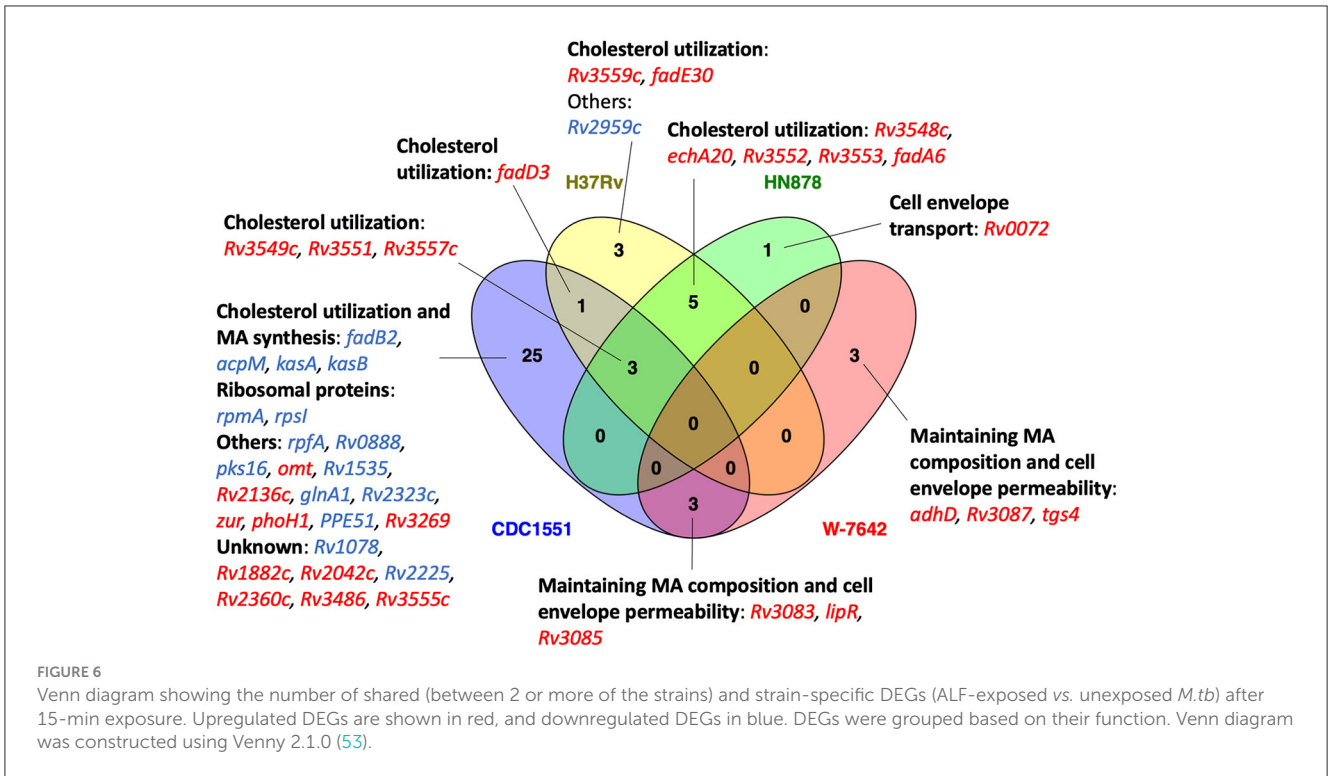
reduced on the *M.tb* cell envelope surface after exposure to human ALF (6), indicating a potential compensatory upregulation of these genes to restore the *M.tb* cell surface. Indeed, *pks1*, involved in the synthesis of immunomodulatory phenolic glycolipids (PGLs) produced by some *M.tb* strains and associated with cell envelope impermeability, phagocytosis, defense against oxidative stress and biofilm formation (46–48), was upregulated in all *M.tb* strains in this study, although was only significant in CDC1551 and W-7642 (Figure 7B, Supplementary Table S3). We note here, though, that many clinical isolates (including CDC1551), as well as laboratory strain H<sub>37</sub>R<sub>v</sub>, contain a *pks1-15* polymorphism associated with the inability of these strains to synthesize PGL (49).

*Rv1685c*, a TetR-like transcriptional regulator that controls an efflux pump with a potential role in the response to acid nitrosative stress (50), was also significantly expressed in HN878 and W-7642 (Figure 7B). Other upregulated genes at 12 h post-ALF exposure were associated to mycobactin assembly (*mtbB*, *mtbC*), involved in iron acquisition, growth in macrophages and virulence (51, 52), and stress response gene *hspX* in H<sub>37</sub>R<sub>v</sub> and HN878, as well as potential immunogenic and virulence-associated genes (*Rv2190c*, *Rv2624c*) in CDC1551 and H<sub>37</sub>R<sub>v</sub>.

We also found several shared downregulated genes after 12-h of ALF exposure (Figure 7A). Genes associated with resistance to aminoglycosides (*acc*, *Rv0263c*, *Rv0264c*) (54), lipid metabolism (*icl1*, *fadB2*) (55), and osmotic stress response and persistence (*Rv0516c*, *mprA*) (56, 57) were consistently downregulated in all four *M.tb* strains. Further, fatty acid (FA) transporter *mmpL12* was down in all *M.tb* strains but CDC1551. We also observed downregulation of mycofactocin synthesis genes, which have a potential multifaceted role in alcohol metabolism of *M.tb*, hypoxia adaptation, and redox homeostasis (58), as well as several lipoproteins and toxin-antitoxin (TA) systems in most of the *M.tb* strains, among others (Figure 7A).

## Strain-specific transcriptional profiles after ALF exposure

In addition to shared transcriptional responses among *M.tb* strains due to ALF exposure, we also observed unique expression signatures attributed to the *M.tb* genomic background at both time points tested, shown in Supplementary Table S5. At 15-min post-ALF exposure, most of the strain-specific DEGs were still related to the KstR2 regulon and maintaining the mycolic acid layer composition and permeability of the *M.tb* cell envelope. We found a gene encoding a probable transmembrane protein responsible for the transport of glutamine across the membrane (*Rv0072*) significantly increased in the hypervirulent HN878 (log<sub>2</sub>FC >5). The highly transmissible CDC1551 showed the most changes at this time point, with 25 unique DEGs (Figure 6). It included downregulation of essential mycolic acid biosynthesis genes *acpM*, *kasA*, and *kasB* (59, 60), *pks16* involved in biofilm formation (61), and cell envelope-associated genes such as *rpfA* (stimulates resuscitation of dormant cells), *Rv0888* (induces formation of neutrophil extracellular traps or NETs) (62), and *glnA1* (regulates nitrogen levels during poly-L-glutamine or PLG synthesis in the cell envelope) (63, 64). Interestingly, a global transcriptional regulator



(*Rv2359* or *zur*) that represses transcription of genes involved in zinc homeostasis was upregulated in CDC1551 (Figure 6).

At 12-h post-ALF exposure, CDC1551 downregulated several cell envelope genes, including *Rv0559c* and *phoY*, with suggested

roles in drug resistance (65, 66). Sigma factor E (*sigE*), involved in persistence to anti-TB drugs and essential for virulence and phagosome maturation in macrophages, was downregulated (67, 68), as well as *msrB*, which encodes a repair enzyme for proteins

that are inactivated by oxidation and reported as upregulated in the resuscitation of dormant *M.tb* (69). In addition, several PE/PPE genes, involved in virulence and the activation of proinflammatory responses, and stress-induced genes (e.g., *hspR*, *clpB*) were also downregulated. In contrast, only a few unique genes were upregulated in CDC1551, including *Rv2958c* and *Rv2959c*, involved in the glycosylation of cell envelope PGLs, and some fatty acid biosynthesis genes, which were initially downregulated at 15-min ALF post-exposure.

Interestingly, H<sub>37</sub>R<sub>v</sub> showed upregulation of several latency-associated *dosR* regulon genes after 12-h of ALF exposure (*Rv2623* or *TB31.7*, *Rv2625c*, *hrp1*) (70), as well as *pncB2*, involved in NAD biosynthesis during host invasion that was found increased during hypoxia (71), indicating a potential role during persistence (Supplementary Table S5). Gene *irtB*, involved in iron homeostasis (72, 73), and a couple of genes associated with resistance to oxidative stress (*lpdA*, *Rv1050*) were also upregulated. Similar to CDC1551, we found two sigma factors with decreased expression (*sigB* and *sigD*), potentially involved in the regulation of the stationary phase of *M.tb* (74). Other unique downregulated genes included *pup*, with a role in proteasomal degradation, and TA-associated genes (Supplementary Table S5).

Of the 28 unique DEGs found in hypervirulent HN878 at 12-h post-ALF exposure, 24 showed significant increased expression ( $\log_2FC > 1$  and  $FDR < 0.1$ ) (Supplementary Table S5). Within the cell envelope functional category, we found *esxI* upregulated, which encodes an ESAT-6 protein secreted by the ESX-5 system that is involved in the virulence of *M.tb* (75). We also found upregulated the lipoprotein *lppJ* of unknown function, and the cluster *Rv1686c/Rv1687c*, a putative efflux pump responsible for the transport of undetermined substrates (potentially drugs) across the membrane that is activated under several environmental stressors (76, 77). Further, unique DEGs from the intermediate metabolism and respiration category were all upregulated in HN878, including *glbN* that encodes an oxygen transport protein upregulated during macrophage infection (78), molybdenum cofactor biosynthesis protein MoaA1, strongly induced under hypoxia (79), and *dxs2*, involved in the mycobacterial ability to prevent acidification of the phagosome (80) (Supplementary Table S5). Contrary to CDC1551 and H<sub>37</sub>R<sub>v</sub>, in HN878 two PE/PPE genes showed increased expression. The only unique downregulated genes in HN878 were two transmembrane proteins of unknown function, an uncharacterized hypothetical protein, and *fadE8*, involved in lipid degradation (Supplementary Table S5).

Finally, MDR-*M.tb* W-7642 showed the most strain-specific DEGs (#155) after 12-h post-ALF exposure compared to unexposed bacteria, with 66 upregulated and 89 downregulated genes (Figure 7). We found upregulation of several genes associated with the ESX-3 system and other genes related to iron acquisition and utilization (*esxH*, *eccD3*, *mycP3*, *Rv0285* or *PE5*, *hemE*, *hemL*, *Rv2047c*), essential for mycobacterial growth *in vitro* and virulence (81) (Supplementary Table S5). In contrast, ESX-1 genes *espD*, *espC*, and *espA* were downregulated. The ESX-1 system secretes host membrane-targeting proteins such as ESAT-6 that interrupt the innate immune response against *M.tb* (82, 83). Other ESAT-6-like proteins were found downregulated (*EsxJ*, *EsxP*, *EsxD*) in W-7642, with the exception of *EsxL* that was upregulated.

Overall, genes generally induced during starvation, persistence, and/or during the stationary phase of *M.tb* showed decreased expression (e.g., *rsbW*, *vapC44*, *mce1R*, *lipU*, *Rv3241c*) (84), as well as sigma factors *sigF* and *sigI* (Supplementary Table S5). However, we observed increased expression of *M.tb* cell envelope biosynthesis genes and lipid metabolism (*Rv2974c*, *aftD*, *murE*, *murF*, *Rv3807c*, *accD6*, *Rv3031*, *kasB*, *acpS*, *fas*, *ppsC*, *ppsD*, *pks15*), amino acid metabolism (*leuC*, *leuD*, *argD*, *trpA*), and DNA repair genes (*ruvB*, *Rv3201c*, *Rv3433c*, *radA*). Interestingly, W-7642 was the only strain with decreased expression of *ethA* (85), but increased expression of *Rv2989* (86), both associated with drug resistance. Other unique DEGs in strain W-7642 are shown in Supplementary Table S5.

RNA-seq results for selected genes of interest were validated by qPCR, showing similar fold change values (Supplementary Figure S4).

## Discussion

Our published studies on the role of ALF during *M.tb* infection indicate that human ALF hydrolases alter the *M.tb* cell envelope, with an impact in subsequent interactions with immune host cells *in vitro* and *in vivo* (6–12). This suggests that physiological levels of ALF play an important role in shaping the *M.tb* cell envelope during the very early stages of infection. Here, we used RNA-seq to depict the transcriptional responses to ALF exposure of four *M.tb* strains with different degrees of transmissibility, virulence, and drug resistance. Our results define for the first time the overall impact of human ALF, first lung component encountered by *M.tb* during infection, on the adaptation of this pathogen to the human alveolar space. We also determined whether exposure to ALF has different transcriptional effects based on the *M.tb* genomic background, which might further define phenotypic differences among *M.tb* strains. Indeed, we observed temporal shared and strain-specific transcriptional responses in *M.tb* after exposure to human ALF, demonstrating that *M.tb* can metabolically adapt to the lung mucosa prior to infecting host cells.

The most striking effect of ALF exposure in the majority of *M.tb* strains studied was the activation of cholesterol utilization pathways, specifically the KstR2 regulon, with some genes induced at 15-min post-ALF exposure and maintained at 12-h (Figure 5). Conversely, expression of genes under the KstR1 regulon remained practically unaltered after exposure to ALF, as well as most of the genes belonging to the Mce3R and SigE regulons (Supplementary Table S3). The ability of *M.tb* to utilize host-derived cholesterol as a source of carbon is essential for survival of *M.tb* in the human host, especially in the nutrient-deprived macrophage environment, where cholesterol significantly contributes to *M.tb* intracellular growth and pathogenesis (37, 87). Indeed, metabolites originated from cholesterol degradation such as pyruvate, acetyl-CoA or succinyl-CoA, can be incorporated into *M.tb* metabolic pathways for cell envelope lipid biosynthesis and production of energy. Further, *M.tb* uses a cholesterol-dependent pathway to infect host cells, induces a foamy macrophage phenotype, and extracts cholesterol and lipids from caseous granulomas to persist, demonstrating the importance of host cholesterol utilization during both early and latent stages of the

infection (88, 89). Importantly, deletion of genes associated with cholesterol catabolism result in attenuated *M.tb* strains (38, 90). Our transcriptomics data suggest that the metabolic adaptation of *M.tb* to use host cholesterol is initiated even before its intracellular stage in host cells, where extracellular *M.tb* starts consuming host cholesterol in the ALF, activating cholesterol degradation pathways that will later be key for infection and survival within host cells. Indeed, cholesterol constitutes most of the neutral lipid in lung surfactant, and levels vary in response to a number of physiological and pathophysiological factors (91–93).

Further, most *M.tb* strains exposed to ALF showed increased expression of some of the genes in the *mymA* operon (*Rv3083–Rv3089*, Supplementary Table S3) after 15-min of contact with ALF (Figure 6). This operon is induced when *M.tb* is exposed to acidic pH and during macrophage infection, demonstrating a role in the modification of fatty acids required for maintaining the appropriate permeability of the cell envelope and mycolic acid layer composition under harsh conditions (44, 45). Furthermore, *mymA* mutants are more susceptible to known anti-TB drugs and detergents, and infection with those mutants results in decreased bacterial load in the spleen of guinea pigs, showing that this operon is also important for *M.tb* pathogenesis and drug resistance (94). This could explain why MDR W-7642 was the only strain in our dataset that had significantly increased expression of all genes from the *mymA* operon after 15-min exposure to ALF. In contrast, *mymA* genes were downregulated at 12-h post-ALF exposure (Figure 7A). These results suggest that, early after contact, *M.tb* upregulates genes that help maintain the cell envelope integrity to compensate for the changes generated upon contact with ALF, but this effect is only temporal and expression of these genes is decreased after a certain period, maybe due to a certain degree of *M.tb* adaptation to the ALF environment. What we know is that ALF exposure to *M.tb* does not affect bacterial viability despite the reported cell envelope (6, 7) and metabolic changes (this study).

In this context, we also found changes in the expression of genes associated to cell envelope biosynthesis and remodeling in ALF-exposed *M.tb*. In fact, we previously reported that *M.tb* exposure to human ALF alters the *M.tb* cell envelope by significantly reducing the total amount of two major *M.tb* cell surface virulence factors, the mannose-capped lipoarabinomannan (ManLAM) and the trehalose dimycolate (TDM), both implicated in promoting phagosome maturation arrest and *M.tb* intracellular growth (5, 6, 46). In response to this reduction, we found in a previous study that *M.tb* Erdman (lineage 4) exposed to ALF upregulated genes involved in the synthesis of TDM and mannose-containing biomolecules (25). We did not observe these same transcriptional effects in ManLAM and TDM in this study, probably due to the fact that different *M.tb* strains were used. However, other cell envelope biosynthesis genes were upregulated by ALF exposure. Indeed, hypervirulent HN878 and MDR W-7642 strains from lineage 2 (Beijing) showed significantly increased expression of DAT/PAT, and SL-1 biosynthesis and transport genes, including MmpL proteins, important for the physiology and pathogenesis of *M.tb* (Figure 7B) (95). Together with ManLAM and TDM, these cell envelope glycolipids have the ability to modulate host cell immune responses (96), as well as blocking phagosome maturation (e.g., fusion with lysosomes) in infected phagocytes (97, 98),

supporting the hypervirulent phenotype found in most Beijing lineage strains.

In addition, other genes involved in the biosynthesis of the *M.tb* cell envelope were significantly upregulated in W-7642, such as *pks1* and *pks15* (PGL synthesis) (48, 49), *murE* and *murF* (peptidoglycan synthesis) (99, 100), *aftD* (biosynthesis of the arabinogalactan region of the *M.tb* cell envelope backbone known as mycolyl-arabinogalactan-peptidoglycan complex or mAGP) (101), *Rv2974c* (hypothetical protein potentially involved in glycerolipid and glycerophospholipid metabolism) (102), and several lipid and amino acid metabolic genes implicated in cell envelope biomass synthesis (99) (Supplementary Table S3). These results indicate that, even though exposure to functional ALF cleaves components of the cell envelope (6), strains HN878 and W-7642 are capable of reprogramming their metabolism and upregulate genes involved in the synthesis of cell surface components involved in *M.tb* survival and pathogenesis (DAT/PAT and SL-1), suggesting a potential lineage-specific response to ALF.

Conversely, other cell envelope-associated genes were significantly downregulated after exposure to ALF for 12-h, including protein export genes in CDC1551 (Supplementary Table S3) and lipoproteins in H<sub>37</sub>Rv, HN878, and especially W-7642. Lipoproteins are membrane-anchored proteins involved in virulence and immunity in *M.tb*, with a dual role, some promote survival of *M.tb* while others induce host protective immune responses (103). The ones found here are some of the less studied, and their specific function/s are still unknown. Interestingly, W-7642 was the only strain with decreased expression of *ethA*, which encodes the enzyme responsible for the activation of the pro-drug ethionamide (85, 104), but increased expression of *Rv2989*, an IclR family transcriptional regulator involved in increased isoniazid tolerance (86). Thus, exposure to ALF might be promoting the drug resistance ability of W-7642, which remains to be elucidated.

ESX or type VII secretion systems, responsible for the secretion of *M.tb* proteins to evade host immune responses (105), were also impacted after 12-h of ALF exposure, especially in MDR W-7642. In this strain, we found significantly increased expression of ESX-3 genes, involved in iron and nutrient uptake and utilization (106), as well as other iron homeostasis genes (e.g., *mtbB*, *mtbC*) important for intracellular growth that were also upregulated in the rest of the strains. In contrast, genes from the ESX-1 system, involved in the lysis of the phagosomal membrane and phagosomal escape of the bacteria (107), were downregulated. Increase of ESX-3 and other iron homeostasis genes after human ALF exposure could be preparing *M.tb* for subsequent infection of macrophages by improving its ability to survive and grow in phagosomes in detriment of other functions (e.g., the ability to escape the phagolysosome). Associated with the ESX-5 secretion system, gene *esxI* (108), suggested to modulate growth in intracellular bacteria, was uniquely upregulated in HN878, potentially related to its hypervirulent genotype.

Several sigma factors (*sigB*, *sigD*, *sigE*, *sigF*, *sigI*) were found downregulated after ALF exposure in all *M.tb* strains studied (significant in all but HN878). Sigma factors are known to contribute to *M.tb* pathogenesis by regulating the expression of genes involved in the adaptation of *M.tb* to stress conditions

encountered during different stages of infection (109), including the stationary phase. Accordingly, the majority of stress response DEGs detected, as well as genes associated to hypoxia and latency, were downregulated in most strains. H<sub>37</sub>R<sub>v</sub> was the exception, showing upregulation of genes with potential roles during persistence and oxidative stress (e.g., *TB31.7*, *hrp1*, *hspX*, *pncB2*, *lpdA*) after exposure to ALF for 12-h (Supplementary Table S5). Overall, this suggests that exposure to ALF might be reducing the ability of some *M.tb* strains (CDC1551, HN878, W-7642) to adapt to long-term survival and persist in a latent state, which remains to be investigated.

Finally, all DEGs from the PE/PPE functional category were downregulated in both CDC1551 and H<sub>37</sub>R<sub>v</sub> after 12-h of exposure to ALF, while some were upregulated in HN878 and W-7642 (Beijing lineage strains) (Supplementary Table S3). While most PE/PPE proteins are still uncharacterized and their molecular mechanisms are unknown, it is suggested that these are involved in *M.tb* virulence and modulation of host immune responses (110). The fact that after exposure to ALF some of these are upregulated only in Beijing lineage strains could indicate a potential adaptive advantage of HN878 and W-7642 to the human host, and suggests again a potential lineage-specific response to ALF. Conversely, TA systems, associated to *M.tb* pathogenicity and persistence (111), were downregulated in most of the *M.tb* strains at 12 h post-ALF exposure, which might be explained by the ALF trying to induce a protective response (6).

In summary, this study shows that human ALF changes the metabolism of *M.tb* in a temporal and strain- and/or lineage-specific manner, and that it is an important environment to consider when studying *M.tb* pathogenesis. Most of the effects were observed at 12-h ALF post-exposure, with the exception of cholesterol utilization pathways that were rapidly upregulated starting at 15-min after exposure. Early exposure (15-min) to ALF also drives upregulation of genes associated with maintaining the appropriate composition of the cell envelope. In addition, our transcriptional analyses show remodeling of the *M.tb* cell envelope, upregulation of genes associated with nutrient and iron uptake (e.g., *ESX-3*), and downregulation of sigma factors and other genes associated with persistence and pathogenesis. These results indicate that the ALF environment promotes changes in *M.tb*'s metabolism, preparing the bacteria for its encounter with host cells (e.g., by upregulating cholesterol utilization pathways and iron/nutrient uptake genes, key for intracellular survival), while at the same time *M.tb* is trying to compensate for ALF-driven changes on the cell envelope early after exposure. In addition, we observed significant differences within strains upon human ALF exposure. Indeed, Beijing lineage strains HN878 and W-7642 upregulated genes associated with the synthesis of cell envelope glycolipids, potentially linked to their hypervirulent phenotype (22, 112).

A limitation of the study is the use of only two replicates from each *M.tb* strain and condition studied for the RNA-seq analysis. Increasing the number of replicates might increase the number of DEGs, especially at 15-min, further confirming our results. However, each replicate consisted of exposing each *M.tb* strain to a pool of 17 different human ALFs, providing us with a good representation of the ALF environment present in healthy participants. We opted for this strategy because using a pool instead of individual ALFs allows us to reduce human variability

and focus on the overall/global effects of ALF exposure in each *M.tb* genotype rather than specific donor ALF-driven changes. Still, we understand that human variability strongly influences the outcomes of the *M.tb* infection and thus, the impact of individual ALFs on *M.tb* metabolism will be further investigated in future studies. In addition, ALF exposure times were selected based on our published data, where changes in the *M.tb* cell envelope were observed in as little as 15-min, with more prominent effects at 12-h (6, 25). Nonetheless, we note that these are not necessarily the most biologically relevant exposure times, since it is currently unknown for how long *M.tb* is in contact with ALF prior to and after infection of alveolar resident and/or compartment cells. What is known is that the recycling of ALF in the alveolar space is every 18 h (26). Thus, future studies will confirm *M.tb* gene expression profiles after longer ALF contact times.

Further, whether the transcriptional changes observed here are strain- and/or lineage-specific remains to be elucidated. This will be further investigated by including genetically close strains from the same lineages (2 and 4) as well as strains from other lineages. Ongoing and future studies will also define the short- and long-term effects of *M.tb* exposure to human ALF *in vitro* and *in vivo*. Regarding the RNA-seq analyses, we decided to use a less stringent FDR value of < 0.1 to capture ALF-driven DEGs that would have been missed otherwise due to only having two replicates/condition, thus increasing the % of potential false positives. Finally, we realize that the metabolic status of *M.tb* grown on agar plates (this study) is unrelated to that of transmitted bacteria. Still, we consider that addressing how *M.tb* adapts metabolically to the first lung environment encountered (ALF) can provide valuable information on the early events of *M.tb* infection, which is still unknown and of major importance in the TB field.

This study provides new insights into specific *M.tb* metabolic pathways affected by exposure to human ALF and further defines transcriptional differences among *M.tb* strains exposed to ALF, highlighting the importance of the alveolar environment and its interactions with *M.tb* during the early infection process, potentially playing a major role in *M.tb* infection and pathogenesis outcomes.

## Data availability statement

All raw and processed sequencing data generated in this study can be found in the NCBI Gene Expression Omnibus (GEO; <https://www.ncbi.nlm.nih.gov/geo/>) (113) under accession number GSE228998.

## Ethics statement

The studies involving humans were approved by the Ohio State University Human Subjects IRB numbers 2008H0135 & 2008H0119 and Texas Biomedical Research Institute/UT-Health San Antonio Human Subjects IRB numbers HSC20170667H & HSC20170315H. The studies were conducted in accordance with the local legislation and institutional requirements. The participants provided their written informed consent to participate in this study.

## Author contributions

AA-G: Conceptualization, Data curation, Formal analysis, Funding acquisition, Investigation, Methodology, Project administration, Supervision, Validation, Visualization, Writing—original draft, Writing—review & editing. AG-V: Formal analysis, Investigation, Visualization, Writing—review & editing. AS: Investigation, Writing—review & editing. AO-F: Investigation, Writing—review & editing. AH: Investigation, Writing—review & editing. JP: Resources, Writing—review & editing. DM: Resources, Writing—review & editing. MW: Resources, Writing—review & editing. YW: Data curation, Writing—review & editing. JT: Conceptualization, Funding acquisition, Methodology, Project administration, Resources, Supervision, Writing—original draft, Writing—review & editing.

## Funding

The author(s) declare financial support was received for the research, authorship, and/or publication of this article. This study was supported by the Robert J. Kleberg Jr. and Helen C. Kleberg Foundation and the National Institute of Allergy and Infectious Diseases of the National Institutes of Health (NIAID/NIH) (award number AI-093570) to JT and the Texas Biomed Forum grant to AA-G. This publication was made possible with help from the Texas Biomed Tuberculosis Research Advancement Center, an NIH-funded program (P30AI168439). RNA sequencing data was generated in the Texas Biomed Molecular Core, which was supported and subsidized by institutional resources and the Genome Sequencing Facility which was supported by UT Health San Antonio, NIH-NCI P30 CA054174 (Cancer Center at UT Health San Antonio) and NIH Shared Instrument grant S10OD030311 (S10 grant to NovaSeq 6000 System), and CPRIT Core Facility Award (RP220662).

## Acknowledgments

Strains CDC1551 (mc<sup>2</sup> 7992 CDC1551 GFP) and W-7642 were a gift from Dr. William R. Jacobs Jr. and Drs. Barry N. Kreiswirth

## References

1. WHO. *Global Tuberculosis Report 2022*. Geneva: WHO. (2022).
2. Hogan AB, Jewell BL, Sherrard-Smith E, Vesga JF, Watson OJ, Whittaker C, et al. Potential impact of the COVID-19 pandemic on HIV, tuberculosis, and malaria in low-income and middle-income countries: a modelling study. *Lancet Glob Health*. (2020) 8:e1132–e41. doi: 10.1016/S2214-109X(20)30288-6
3. Cilloni L, Fu H, Vesga JF, Dowdy D, Pretorius C, Ahmedov S, et al. The potential impact of the COVID-19 pandemic on the tuberculosis epidemic: a modelling analysis. *EClinicalMed*. (2020) 28:100603. doi: 10.1016/j.eclinm.2020.100603
4. Wingfield T, Karmadwala F, MacPherson P, Millington KA, Walker NF, Cuevas LE, et al. Challenges and opportunities to end tuberculosis in the COVID-19 era. *Lancet Respir Med*. (2021) 9:556–8. doi: 10.1016/S2213-2600(21)00161-2
5. Torrelles JB, Schlesinger LS. Integrating lung physiology, immunology, and tuberculosis. *Trends Microbiol*. (2017) 25:688–97. doi: 10.1016/j.tim.2017.03.007

and Barun Mathema, respectively. The following reagent was obtained through BEI Resources, NIAID, NIH: *Mycobacterium tuberculosis*, Strain HN878, NR-13647. We thank Jeremy Glenn and Clinton Christensen at the Texas Biomedical Research Institute Molecular Core for technical support.

## Conflict of interest

The authors declare that the research was conducted in the absence of any commercial or financial relationships that could be construed as a potential conflict of interest.

The author(s) declared that they were an editorial board member of *Frontiers*, at the time of submission. This had no impact on the peer review process and the final decision.

## Publisher's note

All claims expressed in this article are solely those of the authors and do not necessarily represent those of their affiliated organizations, or those of the publisher, the editors and the reviewers. Any product that may be evaluated in this article, or claim that may be made by its manufacturer, is not guaranteed or endorsed by the publisher.

## Author disclaimer

The content is solely the responsibility of the authors and does not necessarily represent the official views of the NIH.

## Supplementary material

The Supplementary Material for this article can be found online at: <https://www.frontiersin.org/articles/10.3389/ftubr.2024.1352806/full#supplementary-material>

6. Arcos J, Sasindran SJ, Fujiwara N, Turner J, Schlesinger LS, Torrelles JB. Human lung hydrolases delineate *Mycobacterium tuberculosis*-macrophage interactions and the capacity to control infection. *J Immunol*. (2011) 187:372–81. doi: 10.4049/jimmunol.1100823
7. Arcos J, Sasindran SJ, Moliva JI, Scordo JM, Sidiki S, Guo H, et al. *Mycobacterium tuberculosis* cell wall released fragments by the action of the human lung mucosa modulate macrophages to control infection in an IL-10-dependent manner. *Mucosal Immunol*. (2017) 10:1248–58. doi: 10.1038/mi.2016.115
8. Arcos J, Diangelo LE, Scordo JM, Sasindran SJ, Moliva JI, Turner J, et al. Lung mucosa lining fluid modification of *mycobacterium tuberculosis* to reprogram human neutrophil killing mechanisms. *J Infect Dis*. (2015) 212:948–58. doi: 10.1093/infdis/jiv146
9. Scordo JM, Arcos J, Kelley HV, Diangelo L, Sasindran SJ, Youngmin E, et al. *Mycobacterium tuberculosis* cell wall fragments released upon bacterial contact with

- the human lung mucosa alter the neutrophil response to infection. *Front Immunol.* (2017) 8:307. doi: 10.3389/fimmu.2017.00307
10. Moliva JL, Duncan MA, Olmo-Fontanez A, Akhter A, Arnett E, Scordo JM, et al. The lung mucosa environment in the elderly increases host susceptibility to mycobacterium tuberculosis infection. *J Infect Dis.* (2019) 220:514–23. doi: 10.1093/infdis/jiz138
11. Scordo JM, Olmo-Fontanez AM, Kelley HV, Sidiki S, Arcos J, Akhter A, et al. The human lung mucosa drives differential Mycobacterium tuberculosis infection outcome in the alveolar epithelium. *Mucosal Immunol.* (2019) 12:795–804. doi: 10.1038/s41385-019-0156-2
12. Olmo-Fontanez AM, Scordo JM, Schami A, Garcia-Vilanova A, Pino PA, Hicks A, et al. Human alveolar lining fluid from the elderly promotes Mycobacterium tuberculosis intracellular growth and translocation into the cytosol of alveolar epithelial cells. *Mucosal Immunol.* (2024). doi: 10.1016/j.mucimm.2024.01.001
13. Moliva JL, Rajaram MV, Sidiki S, Sasindran SJ, Guirado E, Pan XJ, et al. Molecular composition of the alveolar lining fluid in the aging lung. *Age (Dordr).* (2014) 36:9633. doi: 10.1007/s11357-014-9633-4
14. Birhanu AG, Yimer SA, Kalayou S, Riaz T, Zegeye ED, Holm-Hansen C, et al. Ample glycosylation in membrane and cell envelope proteins may explain the phenotypic diversity and virulence in the Mycobacterium tuberculosis complex. *Sci Rep.* (2019) 9:2927. doi: 10.1038/s41598-019-39654-9
15. Howard NC, Marin ND, Ahmed M, Rosa BA, Martin J, Bambouskova M, et al. Mycobacterium tuberculosis carrying a rifampicin drug resistance mutation reprograms macrophage metabolism through cell wall lipid changes (vol 3, pg 1099, 2018). *Nat Microbiol.* (2018) 3:1327. doi: 10.1038/s41564-018-0281-9
16. Velayati AA, Farnia P, Ibrahim TA, Haroun RZ, Kuan HO, Ghanavi J, et al. Differences in cell wall thickness between resistant and nonresistant strains of mycobacterium tuberculosis: using transmission electron microscopy. *Chemotherapy.* (2009) 55:303–7. doi: 10.1159/000226425
17. Pal R, Hameed S, Kumar P, Singh S, Fatima Z. Comparative lipidomics of drug sensitive and resistant Mycobacterium tuberculosis reveals altered lipid imprints. *3 Biotech.* (2017) 7:6. doi: 10.1007/s13205-017-0972-6
18. Allué-Guardia A, Garcia JL, Torrelles JB. Evolution of drug-resistant mycobacterium tuberculosis strains and their adaptation to the human lung environment. *Front Microbiol.* (2021) 12:612675. doi: 10.3389/fmicb.2021.612675
19. Steenken W, Oatway WH, Petroff SA. Biological studies of the tubercle bacillus: III. Dissociation and pathogenicity of the r and s variants of the human tubercle bacillus (H(37)). *J Exp Med.* (1934) 60:515–40. doi: 10.1084/jem.60.4.515
20. Walway SE, Sanchez MP, Shinnick TF, Orme I, Agerton T, Hoy D, et al. An outbreak involving extensive transmission of a virulent strain of Mycobacterium tuberculosis. *N Engl J Med.* (1998) 338:633–9. doi: 10.1056/NEJM199803053381001
21. Subbian S, Bandyopadhyay N, Tsenova L, O'Brien P, Khetani V, Kushner NL, et al. Early innate immunity determines outcome of Mycobacterium tuberculosis pulmonary infection in rabbits. *Cell Commun Signal.* (2013) 11:60. doi: 10.1186/1478-811X-11-60
22. Reed MB, Gagneux S, DeRiemer K, Small PM, Barry CE. The W-Beijing lineage of Mycobacterium tuberculosis overproduces triglycerides and has the DosR dormancy regulon constitutively upregulated. *J Bacteriol.* (2007) 189:2583–9. doi: 10.1128/JB.01670-06
23. Subbian S, Tsenova L, Yang G, O'Brien P, Parsons S, Peixoto B, et al. Chronic pulmonary cavitary tuberculosis in rabbits: a failed host immune response. *Open Biol.* (2011) 1:110016. doi: 10.1098/rsob.110016
24. Bifani PJ, Plikaytis BB, Kapur V, Stockbauer K, Pan X, Lutfey ML, et al. Origin and interstate spread of a New York City multidrug-resistant Mycobacterium tuberculosis clone family. *JAMA.* (1996) 275:452–7. doi: 10.1001/jama.1996.03530300036037
25. Allué-Guardia A, Garcia-Vilanova A, Olmo-Fontanez AM, Peters J, Maselli DJ, Wang Y, et al. Host- and age-dependent transcriptional changes in mycobacterium tuberculosis cell envelope biosynthesis genes after exposure to human alveolar lining fluid. *Int J Mol Sci.* (2022) 23:983. doi: 10.3390/ijms23020983
26. Notter RH. *Lung Surfactants: Basic Science and Clinical Applications.* New York: Marcel Dekker (2000) p. 458.
27. Ames BN. Assay of inorganic phosphate, total phosphate and phosphatases. *Methods Enzymol.* (1966) 8:115–8. doi: 10.1016/0076-6879(66)08014-5
28. Cole ST, Brosch R, Parkhill J, Garnier T, Churcher C, Harris D, et al. Deciphering the biology of Mycobacterium tuberculosis from the complete genome sequence. *Nature.* (1998) 393:537–44. doi: 10.1038/31159
29. Ge SX, Son EW, Yao R. iDEP an integrated web application for differential expression and pathway analysis of RNA-Seq data. *BMC Bioinform.* (2018) 19:534. doi: 10.1186/s12859-018-2486-6
30. Robinson MD, McCarthy DJ, Smyth GK. edgeR: a Bioconductor package for differential expression analysis of digital gene expression data. *Bioinform.* (2010) 26:139–40. doi: 10.1093/bioinformatics/btp616
31. Love MI, Huber W, Anders S. Moderated estimation of fold change and dispersion for RNA-seq data with DESeq2. *Genome Biol.* (2014) 15:550. doi: 10.1186/s13059-014-0550-8
32. Kapopoulou A, Lew JM, Cole ST. The MycoBrowser portal: a comprehensive and manually annotated resource for mycobacterial genomes. *Tuberculosis.* (2011) 91:8–13. doi: 10.1016/j.tube.2010.09.006
33. Ge SX, Jung D, Yao R. ShinyGO: a graphical gene-set enrichment tool for animals and plants. *Bioinformatics.* (2020) 36:2628–9. doi: 10.1093/bioinformatics/btz931
34. Livak KJ, Schmittgen TD. Analysis of relative gene expression data using real-time quantitative PCR and the 2(T)<sup>-</sup>(Delta Delta C) method. *Methods.* (2001) 25:402–8. doi: 10.1006/meth.2001.1262
35. Davis MP, van Dongen S, Abreu-Goodger C, Bartonicek N, Enright AJ. Kraken: a set of tools for quality control and analysis of high-throughput sequence data. *Methods.* (2013) 63:41–9. doi: 10.1016/j.ymeth.2013.06.027
36. Metsalu T, Vilo J. ClustVis: a web tool for visualizing clustering of multivariate data using Principal Component Analysis and heatmap. *Nucleic Acids Res.* (2015) 43:W566–70. doi: 10.1093/nar/gkv468
37. Pawelczyk J, Brzostek A, Minias A, Plocinski P, Rumijowska-Galewicz A, Strapagiel D, et al. Cholesterol-dependent transcriptome remodeling reveals new insight into the contribution of cholesterol to Mycobacterium tuberculosis pathogenesis. *Sci Rep.* (2021) 11:12396. doi: 10.1038/s41598-021-91812-0
38. Crowe AM, Casabon I, Brown KL, Liu J, Lian J, Rogalski JC, et al. Catabolism of the Last Two Steroid Rings in Mycobacterium tuberculosis and Other Bacteria. *mBio.* (2017) 8:17. doi: 10.1128/mBio.00321-17
39. Kendall SL, Burgess P, Balhana R, Withers M, Ten Bokum A, Lott JS, et al. Cholesterol utilization in mycobacteria is controlled by two TetR-type transcriptional regulators: kstR and kstR2. *Microbiology.* (2010) 156:1362–71. doi: 10.1099/mic.0.034538-0
40. Santangelo MP, Klepp L, Nunez-Garcia J, Blanco FC, Soria M, Garcia-Pelayo MDC, et al. Mce3R, a TetR-type transcriptional repressor, controls the expression of a regulon involved in lipid metabolism in Mycobacterium tuberculosis. *Microbiology.* (2009) 155:2245–55. doi: 10.1099/mic.0.027086-0
41. Fontan PA, Aris V, Alvarez ME, Ghanny S, Cheng J, Soteropoulos P, et al. Mycobacterium tuberculosis sigma factor E regulon modulates the host inflammatory response. *J Infect Dis.* (2008) 198:877–85. doi: 10.1086/591098
42. Mohn WW, van der Geize R, Stewart GR, Okamoto S, Liu J, Dijkhuizen L, et al. The actinobacterial mce4 locus encodes a steroid transporter. *J Biol Chem.* (2008) 283:35368–74. doi: 10.1074/jbc.M805496200
43. Gilbert S, Hood L, Seah SYK. Characterization of an aldolase involved in cholesterol side chain degradation in mycobacterium tuberculosis. *J Bacteriol.* (2018) 200:17. doi: 10.1128/JB.00512-17
44. Singh A, Jain S, Gupta S, Das T, Tyagi AK. mymA operon of Mycobacterium tuberculosis: its regulation and importance in the cell envelope. *FEMS Microbiol Lett.* (2003) 227:53–63. doi: 10.1016/S0378-1097(03)00648-7
45. Saraav I, Singh S, Pandey K, Sharma M, Sharma S. Mycobacterium tuberculosis MymA is a TLR2 agonist that activate macrophages and a TH1 response. *Tuberculosis (Edinb).* (2017) 106:16–24. doi: 10.1016/j.tube.2017.05.005
46. Garcia-Vilanova A, Chan J, Torrelles JB. Underestimated manipulative roles of mycobacterium tuberculosis cell envelope glycolipids during infection. *Front Immunol.* (2019) 10:2909. doi: 10.3389/fimmu.2019.02909
47. Pang JM, Layre E, Sweet L, Sherrid A, Moody DB, Ojha A, et al. The polyketide Pks1 contributes to biofilm formation in Mycobacterium tuberculosis. *J Bacteriol.* (2012) 194:715–21. doi: 10.1128/JB.06304-11
48. Ramos B, Gordon SV, Cunha MV. Revisiting the expression signature of pks15/1 unveils regulatory patterns controlling phenolglycerol and phenolglycolipid production in pathogenic mycobacteria. *PLoS ONE.* (2020) 15:e0229700. doi: 10.1371/journal.pone.0229700
49. Constant P, Perez E, Malaga W, Laneelle MA, Saurel O, Daffe M, et al. Role of the pks15/1 gene in the biosynthesis of phenolglycolipids in the Mycobacterium tuberculosis complex. Evidence that all strains synthesize glycosylated p-hydroxybenzoic methyl esters and that strains devoid of phenolglycolipids harbor a frameshift mutation in the pks15/1 gene. *J Biol Chem.* (2002) 277:38148–58. doi: 10.1074/jbc.M206538200
50. Perrone F, De Siena B, Muscariello L, Kendall SL, Waddell SJ, Sacco M, et al. Novel TetR-like transcriptional regulator is induced in acid-nitrosative stress and controls expression of an efflux pump in mycobacteria. *Front Microbiol.* (2017) 8:2039. doi: 10.3389/fmicb.2017.02039
51. Quadri LE, Sello J, Keating TA, Weinreb PH, Walsh CT. Identification of a Mycobacterium tuberculosis gene cluster encoding the biosynthetic enzymes for assembly of the virulence-conferring siderophore mycobactin. *Chem Biol.* (1998) 5:631–45. doi: 10.1016/S1074-5521(98)90291-5
52. Krithika R, Marathe U, Saxena P, Ansari MZ, Mohanty D, Gokhale RS, et al. genetic locus required for iron acquisition in Mycobacterium tuberculosis. *Proc Natl Acad Sci U S A.* (2006) 103:2069–74. doi: 10.1073/pnas.0507924103
53. Oliveros JC. VENN. *An Interactive Tool for Comparing Lists with Venn Diagrams* (2007). Available online at: <https://bioinfogp.cnb.csic.es/tools/venny/index.html>

54. Bassenden AV, Dumalo L, Park J, Blanchet J, Maiti K, Arya DP, et al. Structural and phylogenetic analyses of resistance to next-generation aminoglycosides conferred by AAC(2<sup>r</sup>) enzymes. *Sci Rep.* (2021) 11:11614. doi: 10.1038/s41598-021-89446-3
55. Honer Zu Bentrup K, Miczak A, Swenson DL, Russell DG. Characterization of activity and expression of isocitrate lyase in *Mycobacterium avium* and *Mycobacterium tuberculosis*. *J Bacteriol.* (1999) 181:7161–7. doi: 10.1128/JB.181.23.7161-7167.1999
56. Banerjee SK, Kumar M, Alokam R, Sharma AK, Chatterjee A, Kumar R, et al. Targeting multiple response regulators of *Mycobacterium tuberculosis* augments the host immune response to infection. *Sci Rep.* (2016) 6:25851. doi: 10.1038/srep25851
57. Zahrt TC, Deretic V. *Mycobacterium tuberculosis* signal transduction system required for persistent infections. *Proc Natl Acad Sci U S A.* (2001) 98:12706–11. doi: 10.1073/pnas.221272198
58. Krishnamoorthy G, Kaiser P, Constant P, Abu Abed U, Schmid M, Frese CK, et al. Role of premycofactacin synthase in growth, microaerophilic adaptation, and metabolism of *Mycobacterium tuberculosis*. *MBio.* (2021) 12:e0166521. doi: 10.1128/mBio.01665-21
59. Slayden RA, Barry CE. The role of KasA and KasB in the biosynthesis of meromycolic acids and isoniazid resistance in *Mycobacterium tuberculosis*. *Tuberculosis.* (2002) 82:149–60. doi: 10.1054/tube.2002.0333
60. Yuan Y, Mead D, Schroeder BG, Zhu Y, Barry CE. The biosynthesis of mycolic acids in *Mycobacterium tuberculosis* Enzymatic methyl(ene) transfer to acyl carrier protein bound meromycolic acid in vitro. *J Biol Chem.* (1998) 273:21282–90. doi: 10.1074/jbc.273.33.21282
61. Ojha AK, Baughn AD, Sambandan D, Hsu T, Trivelli X, Guerardel Y, et al. Growth of *Mycobacterium tuberculosis* biofilms containing free mycolic acids and harbouring drug-tolerant bacteria. *Mol Microbiol.* (2008) 69:164–74. doi: 10.1111/j.1365-2958.2008.06274.x
62. Dang G, Cui Y, Wang L, Li T, Cui Z, Song N, et al. Extracellular sphingomyelinase Rv0888 of *Mycobacterium tuberculosis* contributes to pathological lung injury of *Mycobacterium smegmatis* in mice via inducing formation of neutrophil extracellular traps. *Front Immunol.* (2018) 9:677. doi: 10.3389/fimmu.2018.00677
63. Tripathi D, Chandra H, Bhatnagar R. Poly-L-glutamate/glutamine synthesis in the cell wall of *Mycobacterium bovis* is regulated in response to nitrogen availability. *BMC Microbiol.* (2013) 13:226. doi: 10.1186/1471-2180-13-226
64. Harth G, Clemens DL, Horwitz MA. Glutamine synthetase of *Mycobacterium tuberculosis*: extracellular release and characterization of its enzymatic activity. *Proc Natl Acad Sci U S A.* (1994) 91:9342–6. doi: 10.1073/pnas.91.20.9342
65. Gamngoen R, Putim C, Salee P, Phunpae P, Butr-Indr B. A comparison of Rv0559c and Rv0560c expression in drug-resistant *Mycobacterium tuberculosis* in response to first-line antituberculosis drugs. *Tuberculosis (Edinb).* (2018) 108:64–9. doi: 10.1016/j.tube.2017.11.002
66. Wang C, Mao Y, Yu J, Zhu L, Li M, Wang D, et al. PhoY2 of mycobacteria is required for metabolic homeostasis and stress response. *J Bacteriol.* (2013) 195:243–52. doi: 10.1128/JB.01556-12
67. Pisu D, Proveddi R, Espinosa DM, Payan JB, Boldrin F, Palu G, et al. The alternative sigma factors SigE and SigB are involved in tolerance and persistence to antitubercular drugs. *Antimicrob Agents Chemother.* (2017) 61:12. doi: 10.1128/AAC.01596-17
68. Casonato S, Proveddi R, Dainese E, Palu G, Manganelli R. *Mycobacterium tuberculosis* requires the ECF sigma factor SigE to arrest phagosome maturation. *PLoS ONE.* (2014) 9:e108893. doi: 10.1371/journal.pone.0108893
69. Salina EG, Grigorov AS, Bychenko OS, Skvortsova YV, Mamedov IZ, Azhikina TL, et al. Resuscitation of dormant “non-culturable” *Mycobacterium tuberculosis* is characterized by immediate transcriptional burst. *Front Cell Infect Microbiol.* (2019) 9:272. doi: 10.3389/fcimb.2019.00272
70. Garcia-Morales L, Leon-Solis L, Monroy-Munoz IE, Talavera-Paulin M, Serafin-Lopez J, Estrada-Garcia I, et al. Comparative proteomic profiles reveal characteristic *Mycobacterium tuberculosis* proteins induced by cholesterol during dormancy conditions. *Microbiology.* (2017) 163:1237–47. doi: 10.1099/mic.0.000512
71. Boshoff HI, Xu X, Tahlhan K, Dowd CS, Pethe K, Camacho LR, et al. Biosynthesis and recycling of nicotinamide cofactors in *Mycobacterium tuberculosis*. An essential role for NAD in nonreplicating bacilli. *J Biol Chem.* (2008) 283:19329–41. doi: 10.1074/jbc.M800694200
72. Zhang L, Hendrickson RC, Meikle V, Lefkowitz EJ, Ioerger TR, Niederweis M. Comprehensive analysis of iron utilization by *Mycobacterium tuberculosis*. *PLoS Pathog.* (2020) 16:e1008337. doi: 10.1371/journal.ppat.1008337
73. Rodriguez GM, Smith I. Identification of an ABC transporter required for iron acquisition and virulence in *Mycobacterium tuberculosis*. *J Bacteriol.* (2006) 188:424–30. doi: 10.1128/JB.188.2.424-430.2006
74. Chauhan R, Ravi J, Datta P, Chen T, Schnappinger D, Bassler KE, et al. Reconstruction and topological characterization of the sigma factor regulatory network of *Mycobacterium tuberculosis*. *Nat Commun.* (2016) 7:11062. doi: 10.1038/ncomms11062
75. Shah S, Cannon JR, Fenselau C, Briken V. A duplicated ESAT-6 region of ESX-5 is involved in protein export and virulence of mycobacteria. *Infect Immun.* (2015) 83:4349–61. doi: 10.1128/IAI.00827-15
76. Birhanu AG, Gomez-Munoz M, Kalayou S, Riaz T, Lutter T, Yimer SA, et al. Proteome profiling of *Mycobacterium tuberculosis* cells exposed to nitrosative stress. *ACS Omega.* (2022) 7:3470–82. doi: 10.1021/acsomega.1c05923
77. Machado D, Couto I, Perdigao J, Rodrigues L, Portugal I, Baptista P, et al. Contribution of efflux to the emergence of isoniazid and multidrug resistance in *Mycobacterium tuberculosis*. *PLoS ONE.* (2012) 7:e34538. doi: 10.1371/journal.pone.0034538
78. Couture M, Yeh SR, Wittenberg BA, Wittenberg JB, Ouellet Y, Rousseau DL, et al. A cooperative oxygen-binding hemoglobin from *Mycobacterium tuberculosis*. *Proc Natl Acad Sci U S A.* (1999) 96:11223–8. doi: 10.1073/pnas.96.20.11223
79. Levillain F, Poquet Y, Mallet L, Mazeres S, Marceau M, Brosch R, et al. Horizontal acquisition of a hypoxia-responsive molybdenum cofactor biosynthesis pathway contributed to *Mycobacterium tuberculosis* pathoadaptation. *PLoS Pathog.* (2017) 13:e1006752. doi: 10.1371/journal.ppat.1006752
80. Pethe K, Swenson DL, Alonso S, Anderson J, Wang C, Russell DG. Isolation of *Mycobacterium tuberculosis* mutants defective in the arrest of phagosome maturation. *Proc Natl Acad Sci U S A.* (2004) 101:13642–7. doi: 10.1073/pnas.0401657101
81. Siegrist MS, Unnikrishnan M, McConnell MJ, Borowsky M, Cheng TY, Siddiqi N, et al. *Mycobacterial* Esx-3 is required for mycobactin-mediated iron acquisition. *Proc Natl Acad Sci U S A.* (2009) 106:18792–7. doi: 10.1073/pnas.0900589106
82. Wong KW. The Role of ESX-1 in *Mycobacterium tuberculosis* Pathogenesis. *Microbiol Spectr.* (2017) 5:3. doi: 10.1128/microbiolspec.TB2-0001-2015
83. Hsu T, Hingley-Wilson SM, Chen B, Chen M, Dai AZ, Morin PM, et al. The primary mechanism of attenuation of bacillus Calmette-Guérin is a loss of secreted lytic function required for invasion of lung interstitial tissue. *P Natl Acad Sci USA.* (2003) 100:12420–5. doi: 10.1073/pnas.1635213100
84. Hampshire T, Soneji S, Bacon J, James BW, Hinds J, Laing K, et al. Stationary phase gene expression of *Mycobacterium tuberculosis* following a progressive nutrient depletion: a model for persistent organisms? *Tuberculosis.* (2004) 84:228–38. doi: 10.1016/j.tube.2003.12.010
85. Dover LG, Alahari A, Gratraud P, Gomes JM, Bhowruth V, Reynolds RC, et al. EthA, a common activator of thiocarbamide-containing drugs acting on different mycobacterial targets. *Antimicrob Agents Chemother.* (2007) 51:1055–63. doi: 10.1128/AAC.01063-06
86. Li QF, Li T, Fan C, Xie X. Mycobacterial IclR family transcriptional factor Rv2989 is specifically involved in isoniazid tolerance by regulating the expression of catalase encoding gene *katG*. *RCS Adv.* (2016) 6:54661–7. doi: 10.1039/C6RA07733A
87. Brzostek A, Pawelczyk J, Rumijowska-Galewicz A, Dziadek B, Dziadek J. *Mycobacterium tuberculosis* is able to accumulate and utilize cholesterol. *J Bacteriol.* (2009) 191:6584–91. doi: 10.1128/JB.00488-09
88. Peyron P, Vaubourgeix J, Poquet Y, Levillain F, Botanch C, Bardou F, et al. Foamy macrophages from tuberculous patients’ granulomas constitute a nutrient-rich reservoir for *M. tuberculosis* persistence. *PLoS Pathog.* (2008) 4:e1000204. doi: 10.1371/journal.ppat.1000204
89. Pandey AK, Sasseti CM. Mycobacterial persistence requires the utilization of host cholesterol. *Proc Natl Acad Sci U S A.* (2008) 105:4376–80. doi: 10.1073/pnas.0711159105
90. Hu Y, van der Geize R, Besra GS, Gurcha SS, Liu A, Rohde M, et al. 3-Ketosteroid 9alpha-hydroxylase is an essential factor in the pathogenesis of *Mycobacterium tuberculosis*. *Mol Microbiol.* (2010) 75:107–21. doi: 10.1111/j.1365-2958.2009.06957.x
91. Fessler MB. A new frontier in immunometabolism. cholesterol in lung health and disease. *Ann Am Thorac Soc.* (2017) 14:S399–S405. doi: 10.1513/AnnalsATS.201702-136AW
92. Agudelo CW, Samaha G, Garcia-Arcos I. Alveolar lipids in pulmonary disease. A review. *Lipids Health Dis.* (2020) 19:122. doi: 10.1186/s12944-020-01278-8
93. Sallèse A, Suzuki T, McCarthy C, Bridges J, Filuta A, Arumugam P, et al. Targeting cholesterol homeostasis in lung diseases. *Sci Rep.* (2017) 7:10211. doi: 10.1038/s41598-017-10879-w
94. Singh A, Gupta R, Vishwakarma RA, Narayanan PR, Paramasivan CN, Ramanathan VD, et al. Requirement of the *mymA* operon for appropriate cell wall ultrastructure and persistence of *Mycobacterium tuberculosis* in the spleens of guinea pigs. *J Bacteriol.* (2005) 187:4173–86. doi: 10.1128/JB.187.12.4173-4186.2005
95. Melly G, Purdy GE. MmpL proteins in physiology and pathogenesis of *M. tuberculosis*. *Microorganisms.* (2019) 7:70. doi: 10.3390/microorganisms7030070
96. Zhang L, English D, Andersen BR. Activation of human neutrophils by *Mycobacterium tuberculosis*-derived sulfolipid-1. *J Immunol.* (1991) 146:2730–6. doi: 10.4049/jimmunol.146.8.2730
97. Brodin P, Poquet Y, Levillain F, Peguillet I, Larrouy-Maumus G, Gilleron M, et al. High content phenotypic cell-based visual screen identifies *Mycobacterium tuberculosis* acyltrehalose-containing glycolipids involved in phagosome remodeling. *PLoS Pathog.* (2010) 6:e1001100. doi: 10.1371/journal.ppat.1001100
98. Gilmore SA, Schelle MW, Holsclaw CM, Leigh CD, Jain M, Cox JS, et al. Sulfolipid-1 biosynthesis restricts *Mycobacterium tuberculosis* growth in human macrophages. *ACS Chem Biol.* (2012) 7:863–70. doi: 10.1021/cb200311s

99. Maitra A, Munshi T, Healy J, Martin LT, Vollmer W, Keep NH, et al. Cell wall peptidoglycan in *Mycobacterium tuberculosis*: an Achilles' heel for the TB-causing pathogen. *FEMS Microbiol Rev.* (2019) 43:548–75. doi: 10.1093/femsre/fuz016
100. Basavannacharya C, Moody PR, Munshi T, Cronin N, Keep NH, Bhakta S. Essential residues for the enzyme activity of ATP-dependent MurE ligase from *Mycobacterium tuberculosis*. *Protein Cell.* (2010) 1:1011–22. doi: 10.1007/s13238-010-0132-9
101. Skovierova H, Larrouy-Maumus G, Zhang J, Kaur D, Barilone N, Kordulakova J, et al. AftD, a novel essential arabinofuranosyltransferase from mycobacteria. *Glycobiology.* (2009) 19:1235–47. doi: 10.1093/glycob/cwp116
102. Vargas R, Freschi L, Marin M, Epperson LE, Smith M, Oussenko I, et al. In-host population dynamics of *Mycobacterium tuberculosis* complex during active disease. *Elife.* (2021) 10:e61805. doi: 10.7554/eLife.61805
103. Becker K, Sander P. *Mycobacterium tuberculosis* lipoproteins in virulence and immunity - fighting with a double-edged sword. *FEBS Lett.* (2016) 590:3800–19. doi: 10.1002/1873-3468.12273
104. Baulard AR, Betts JC, Engohang-Ndong J, Quan S, McAdam RA, Brennan PJ, et al. Activation of the pro-drug ethionamide is regulated in mycobacteria. *J Biol Chem.* (2000) 275:28326–31. doi: 10.1074/jbc.M003744200
105. Groschel MI, Sayes F, Simeone R, Majlessi L, Brosch R, ESX. secretion systems: mycobacterial evolution to counter host immunity. *Nat Rev Microbiol.* (2016) 14:677–91. doi: 10.1038/nrmicro.2016.131
106. Tufariello JM, Chapman JR, Kerantzas CA, Wong KW, Vilcheze C, Jones CM, et al. Separable roles for *Mycobacterium tuberculosis* ESX-3 effectors in iron acquisition and virulence. *Proc Natl Acad Sci U S A.* (2016) 113:E348–57. doi: 10.1073/pnas.1523321113
107. Conrad WH, Osman MM, Shanahan JK, Chu F, Takaki KK, Cameron J, et al. *Mycobacterium tuberculosis* ESX-1 secretion system mediates host cell lysis through bacterium contact-dependent gross membrane disruptions. *Proc Natl Acad Sci U S A.* (2017) 114:1371–6. doi: 10.1073/pnas.1620133114
108. Bukka A, Price CT, Kernodle DS, Graham JE. *Mycobacterium tuberculosis* RNA expression patterns in sputum bacteria indicate secreted *esx* factors contributing to growth are highly expressed in active disease. *Front Microbiol.* (2011) 2:266. doi: 10.3389/fmicb.2011.00266
109. Sachdeva P, Misra R, Tyagi AK, Singh Y. The sigma factors of *Mycobacterium tuberculosis*: regulation of the regulators. *FEBS J.* (2010) 277:605–26. doi: 10.1111/j.1742-4658.2009.07479.x
110. Ates LS. New insights into the mycobacterial PE and PPE proteins provide a framework for future research. *Mol Microbiol.* (2020) 113:4–21. doi: 10.1111/mmi.14409
111. Yu X, Gao X, Zhu K, Yin H, Mao X, Wojdyla JA, et al. Characterization of a toxin-antitoxin system in *Mycobacterium tuberculosis* suggests neutralization by phosphorylation as the antitoxicity mechanism. *Commun Biol.* (2020) 3:216. doi: 10.1038/s42003-020-0941-1
112. Huet G, Constant P, Malaga W, Laneelle MA, Kremer K, van Soolingen D, et al. A lipid profile typifies the Beijing strains of *Mycobacterium tuberculosis*: identification of a mutation responsible for a modification of the structures of phthiocerol dimycocerosates and phenolic glycolipids. *J Biol Chem.* (2009) 284:27101–13. doi: 10.1074/jbc.M109.041939
113. Edgar R, Domrachev M, Lash AE. Gene Expression Omnibus: NCBI gene expression and hybridization array data repository. *Nucleic Acids Res.* (2002) 30:207–10. doi: 10.1093/nar/30.1.207